

REVIEW

DETECTION OF PERITONEAL METASTASES

Jeremiah C. Healy

*Corresponding author: Dr Jeremiah C Healy, Chelsea and Westminster Hospital,
369 Fulham Road, London SW10 9NH UK*

ABSTRACT

The peritoneum is the largest and most complexly arranged serous membrane in the body. The potential peritoneal spaces, the peritoneal reflections forming peritoneal ligaments, mesenteries, omenta, and the natural flow of peritoneal fluid determine the route of spread of intraperitoneal fluid and consequently disease spread within the abdominal cavity. The peritoneal ligaments, mesenteries, and omenta also serve as boundaries and conduits for disease spread. Peritoneal metastases spread in four ways:

- Direct spread along peritoneal ligaments, mesenteries and omenta to non-contiguous organs;
- Intraperitoneal seeding via ascitic fluid;
- Lymphatic extension;
- Embolic haematogenous spread.

Before the introduction of cross-sectional imaging, the peritoneum and its reflections could only be imaged with difficulty, often requiring invasive techniques. Computed tomography and to a lesser extent sonography and MR imaging allow us to examine the complex anatomy of the peritoneal cavity accurately, which is the key to understanding the spread of peritoneal metastases. This article reviews the detection of peritoneal metastases.

INTRODUCTION

The peritoneal cavity is the potential space between the visceral and parietal layers of the peritoneum. The parietal peritoneum is reflected over the peritoneal organs to form a series of supporting ligaments, mesenteries and omenta (Fig. 1). These peritoneal reflections act as a natural pathway for the dissemination of intra-abdominal disease within the peritoneum, but also allow extension of disease from the retroperitoneum to structures enveloped by peritoneum, via the subperitoneal space^[1].

Metastatic disease is the most common malignant process involving the peritoneum. Metastases are usually from intra-abdominal primary neoplasms, such as carcinoma of the stomach, colon, ovary and pancreas, or from intraabdominal lymphoma.



Figure 1 Diagrammatic representation of the peritoneal anatomy. (a) Coronal view of the posterior peritoneal spaces. (b) Coronal view of the peritoneal attachments to the abdominal wall.

Prior to the advent of CT, peritoneal metastases were not radiographically detectable until late in the disease, when they displaced adjacent organs, caused intestinal obstruction, or produced radiological signs due to massive ascites on plain films. CT can identify peritoneal metastases as small as a few millimetres in size and also identify very small volumes of ascites. This information is essential in staging tumours, assessing resectability, monitoring response, and identifying recurrence.

The imaging appearances of metastatic peritoneal disease are in part determined by the tumour type itself, but predominantly by the mode of peritoneal dissemination.

IMAGING TECHNIQUES

Computed tomography

CT is considered the best imaging procedure for the evaluation of patients with known or suspected peritoneal metastases. The use of intraperitoneal positive contrast and pneumoperitoneum with CT has been suggested to improve the detection of small peritoneal metastases but these techniques do not routinely opacify all the peritoneal recesses^[2-4]. These methods are more interventional and time consuming and consequently are not widely used.

MR Imaging

Recent reports describe the use of MR imaging in identifying peritoneal implants^[5,6]. MR imaging of the peritoneum has been most successfully achieved using fat saturated T1-weighted sequences following intravenous gadolinium^[7]. The inferior spatial resolution, the problems of motion artefact related to respiration and bowel peristalsis, and the lack of an effective bowel opacification agent makes MR imaging a generally less accurate test than CT for the identification of peritoneal metastases. However a recent report from the Radiological Diagnostic Oncology Group^[8] reviewed the performance of ultrasound, MR imaging, and CT for diagnosing and staging ovarian cancer. They found in a group of 280 patients that CT and MR imaging had similar accuracy for staging advanced ovarian cancer. Both were much more accurate than ultrasound.

This study used state-of-the-art MR techniques with phased array body coils, breath-hold sequences which included T1-weighted images with fat saturation before and after intravenous gadolinium chelate.

Ultrasound

Ultrasound will demonstrate superficial peritoneal and omental metastases as small as 2 to 3 mm in the presence of ascites. However, centrally located deposits, for example in the small mesentery, will not be visualized because of the acoustic impedance of bowel gas and fat^[9,10]. Ultrasound is useful for image-guided aspiration/drainage of ascites and the biopsy of superficial peritoneal deposits.

Barium studies

Barium studies provide only indirect signs of peritoneal and mesenteric disease and thus are not used as the first line of investigation. The typical features of mesenteric or omental infiltration by metastases include: mass effect on adjacent bowel; nodularity, spiculation or tethering of adjacent mucosal folds or haustra; sacculation of the uninvolved contralateral border; or circumferential

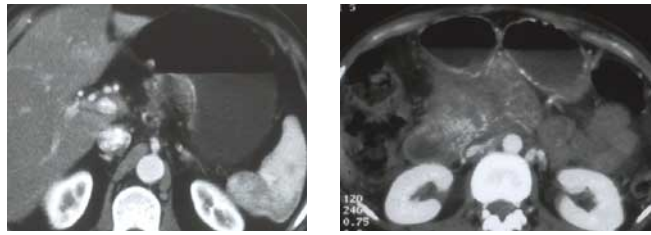


Figure 2 Direct spread of metastatic deposits in the lesser omentum/transverse mesocolon. (a) Axial post contrast CT scan in a 59-year-old male with gastric cancer showing extension of gastric cancer into the lesser omental fat. (b) Axial post contrast CT scan in a 45-year-old female with carcinoma of the pancreatic body with metastatic extension in the transverse mesocolon causing bowel obstruction.

narrowing of the bowel lumen. These changes most frequently occur with contiguous involvement of the transverse colon or stomach. Barium studies will occasionally reveal abnormalities related to peritoneal metastases not clearly demonstrated on CT.

Scintigraphy

Scintigraphy has also been used to identify peritoneal metastases but is not very sensitive or specific and needs CT for anatomical location^[11].

MODES OF SPREAD AND IMAGING APPEARANCES

Metastases spread throughout the peritoneum in four ways:

- directly along peritoneal ligaments, mesenteries and omenta to non-contiguous structures;
- intraperitoneal seeding via the flow of ascitic fluid;
- lymphatic extension;
- embolic haematogenous spread^[12].

Direct spread

Direct invasion from primary tumours to noncontiguous organs occurs along the peritoneal reflections (Fig. 1b). These include:

- Eight ligaments — the right and left coronary, falciform, hepatoduodenal, duodenocolic, gastrosplenic, splenorenal, and phrenicocolic ligaments;
- Four mesenteries — the small bowel mesentery, the transverse mesocolon, the sigmoid mesocolon, and the mesoappendix;
- Two omenta — the lesser and greater omentum^[12,13].

Spread along these peritoneal reflections is commonly seen with malignant neoplasms of the stomach, colon, pancreas and ovary.

CT appearances

Carcinoma of the stomach often spreads directly into the left lobe of the liver via the lesser omentum, extending between the lesser curvature of the stomach and the liver (Fig. 2a)^[14]. CT shows loss of the fat plane between these two organs^[15]. Direct spread from retroperitoneal tumours, such as carcinoma of the pancreas, into the liver can occur along the hepatoduodenal ligament, which is the free edge of the lesser omentum, extending from the junction of the first and second parts of the duodenum to the porta hepatis^[16,17]. Biliary and hepatic malignancies can also spread in the reverse direction to the stomach and pancreas via the lesser omentum and hepatoduodenal ligaments. On CT these masses are often hypervascular and may have low attenuation centrally due to central necrosis^[18,19].

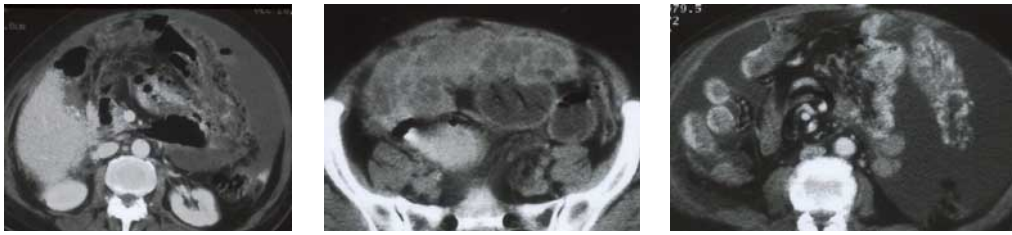


Figure 3 Metastatic deposits in the greater omentum. (a) Post contrast axial CT scan in a 49-year-old female with carcinoma of the ovary showing several nodular, ill defined masses in the greater omentum anterior to the colon. Note also the ascites. (b) Axial post contrast CT scan in a 66-year-old female with adenocarcinoma of the bowel showing a bulky, 'cake-like', enhancing omental deposit. (c) Axial post contrast CT scan in a 65-year-old male patient with renal carcinoma showing markedly enhancing deposits within the greater omentum surrounded by ascites. Note also enhancing serosal deposits on the surface of the bowel.

Neoplasms of the colon, stomach, and pancreas often use the transverse mesocolon and greater omentum as conduits for spread (Fig. 2b). Direct invasion is well demonstrated on CT as increased density or discrete soft tissue masses in the fat of the transverse mesocolon. The right hand margin of the transverse mesocolon is thickened as the duodenocolic ligament providing a direct route for extension of colonic cancer from the hepatic flexure to the duodenum^[20.21].

The greater omentum extends from the greater curve of the stomach and suspends the transverse colon. On CT early involvement of the greater omentum produces increased density within the fat adjacent to the primary neoplasm (Fig. 3a). Subsequently, masses contiguous with the primary neoplasm may be seen extending into the greater omentum, producing 'omental caking', which separates the colon from the anterior abdominal wall (Fig. 3b.). Spread of metastatic disease along the left-hand margin of the greater omentum stops abruptly at the phrenicocolic ligament, extending from the splenic flexure to the diaphragm. It marks the point at which the mesenteric transverse colon becomes the extraperitoneal descending colon.

In the left upper quadrant the gastrosplenic ligament, continuous with the greater omentum, extends from the greater curve of the stomach to the spleen. It can be involved by extramural spread from gastric cancer and explains the association of splenic abscess with this tumour, often seen on CT^[22].

Direct involvement of the small bowel mesentery is commonly seen in carcinoid (Fig. 4), lymphoma, pancreatic, breast and colonic metastases. Spread from the retroperitoneum, via the subperitoneal space, to the small bowel is frequently seen in lymphoma. On CT, this produces soft tissue thickening within the mesenteric fat, perivascular encasement and tethering of the bowel.

Intraperitoneal seeding

Intraperitoneal fluid is constantly circulating throughout the abdomen influenced by gravity and negative intraabdominal pressure, produced beneath the diaphragm during respiration. It allows transcoelomic dissemination of malignant cells. Their deposition, fixation and growth are encouraged in particular sites due to relative stasis of ascitic fluid^[23].

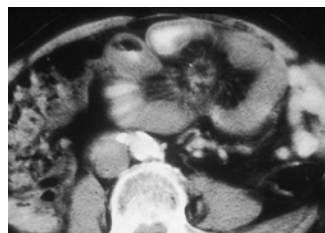


Figure 4 Small bowel mesenteric deposits. Post contrast axial CT scan in a 28-year-old female with carcinoid tumour of the terminal ileum. Note the mesenteric mass at the root of the small bowel mesentery and linear soft tissue stranding and tethering in the small bowel mesenteric fat.

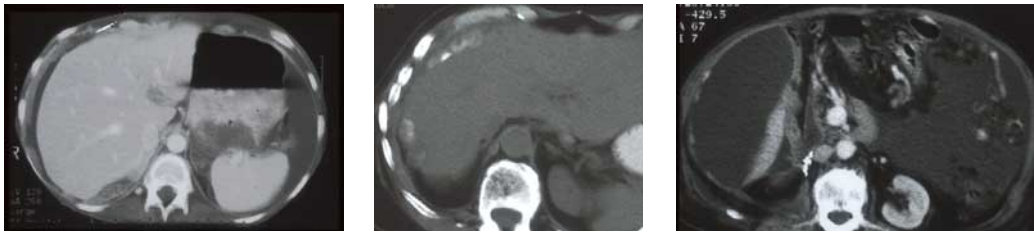


Figure 5 Intraperitoneal seeding of peritoneal metastases. (a) Axial post contrast CT scan in a 49-year-old female with carcinoma of the ovary demonstrating nodular parietal peritoneal thickening, in association with a deposit in Morison's pouch, and ascites. (b) Axial CT scan in a 66-year-old female with carcinoma of the ovary showing calcified peritoneal metastases. (c) Axial post contrast CT scan in the same patient as in Fig. 3A. Note the clips from previous renal surgery. Multiple enhancing peritoneal metastases are outlined by ascites. Note also enhancing deposits in the greater omental fat.

The most common tumours to spread in this fashion include ovarian cancer in females and malignancies of the gastrointestinal tract in males, especially cancer of the stomach, colon, and pancreas.

The sites most commonly involved by peritoneal seeding are (Fig. 1a):

- the pelvis, especially the pouch of Douglas;
- the right lower quadrant at the inferior junction of the small bowel mesentery;
- the superior aspect of the sigmoid mesocolon;
- the right paracolic gutter^[23].

Spread of deposits to the right subhepatic and subphrenic spaces is also frequently seen, especially in ovarian cancer. Almost 90% of patients with ovarian cancer have peritoneal implants at post mortem and 60–70% have ascites^[24,25].

CT appearances. On CT, seeded metastases appear as nodular or plaque-like soft tissue masses in association with ascites. Intraperitoneal deposits as small as 5 mm can be identified, even in the presence of small amounts of ascites^[26–28]. Rounded or oval low density deposits on the surface of the liver are frequently seen on CT in ovarian cancer (Fig. 5a)^[29]. These are generally of 0.5–1 cm diameter located on the dorsomedial and dorsolateral parts of the right lobe of the liver and often associated with deposits in Morison's pouch (Fig. 5a). It is presumed that these deposits infiltrate the liver capsule following their deposition on the liver surface. The parietal peritoneum may be diffusely involved producing smooth or nodular thickening (Fig. 5a) on CT that often enhances (Fig. 5c)^[30]. Peritoneal calcification is also frequently seen on CT with serous cystadenocarcinoma of the ovary (Fig. 5b), carcinoid tumour, and rarely with gastric carcinoma^[31–33].

A distinctive CT appearance is produced by *pseudomyxoma peritonei*, resulting from the rupture of a mucinous cystadenocarcinoma or cystadenoma of the ovary or appendix (Fig. 6a,b). The gelatinous nature of the deposits produces a mantle of low density material over the surface of the liver, causing scalloping of its margin, in association with cystic peritoneal collections (Fig. 6a). The walls of the cystic collections may contain calcification. The pressure of the gelatinous material

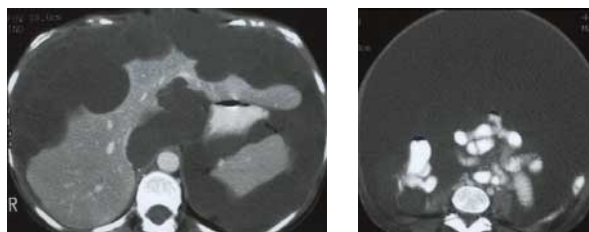


Figure 6 Pseudomyxoma peritonei in mucinous cystadenocarcinoma of the appendix in a 44-year-old female. (a) Axial post contrast CT scans showing low density deposits producing scalloping of the liver margin. (b) The pressure of the gelatinous material prevents bowel loops floating up towards the anterior abdominal wall.

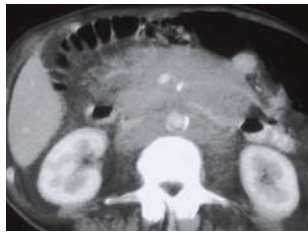


Figure 7 Lymphatic metastases. 45-year-old male patient with Non-Hodgkins Lymphoma showing the characteristic 'Sandwich' sign of mesenteric and retroperitoneal lymph node involvement.

prevents the bowel loops floating up towards the anterior abdominal wall, which may be a useful sign in differentiating *pseudomyxoma peritonei* from ascites (Fig. 6b)^[34].

The small bowel mesentery and greater omentum are frequently involved by intraperitoneal seeding of metastases. Four patterns of involvement are described on CT: round masses, 'cake-like' masses (Fig. 3b), ill-defined masses, and stellate masses^[35].

Irregular, 'cake-like' masses are seen most often with ovarian cancer^[36]. Densely calcified omental 'cake' has been reported in metastatic serous cystadenocarcinoma^[37]. The stellate pattern of mesenteric or omental mass is seen with pancreatic, colonic and breast cancer and results from diffuse infiltration, causing thickening and rigidity of the perivascular bundles. Widespread peritoneal metastases, including omental infiltration is a rare consequence of retroperitoneal malignancy, such as renal cell carcinoma (Fig. 3c, 5c)^[38].

Metastatic deposits to the ovaries from gastric or colonic primary tumours in association with ascites and other peritoneal deposits are a well-recognized entity. These tumours, known as '*Krukenberg*' tumours, are presumed to be a consequence of transcoelomic spread and are clearly visualized on CT^[39].

Lymphatic metastases

Lymphatic metastases play a minor role in the intraperitoneal dissemination of metastatic carcinoma, but is very important in the spread of lymphoma to mesenteric lymph nodes. Almost 50% of patients with non-Hodgkin's lymphoma will have mesenteric nodes at presentation, compared to only 5% of patients with Hodgkin's disease^[40]. On CT, mesenteric lymph node involvement in lymphoma produces round or oval masses in the mesenteric fat, which may displace adjacent loops of bowel^[35]. Large conglomerations of lymph nodes may surround the superior mesenteric artery and vein on CT and demonstrate the so-called 'sandwich sign' (Fig. 7) where lymphomatous mesenteric masses are separated from retroperitoneal lymphadenopathy by an intact anterior pararenal fat plane^[35,41].

Embolic metastases

The abdomen is a common site for haematogenous metastases from both intra-abdominal and extra-abdominal primary tumours. The tumour emboli spread via the mesenteric arteries to deposit on the antimesenteric border of the bowel in the smallest arterial branches, where they grow into mural nodules.

The most common tumours that metastasise embolically to bowel and the peritoneal reflections are melanoma, breast and lung cancer. These metastases often occur several years after treatment of the primary neoplasm. Occasionally bowel obstruction or intussusception, as a consequence of embolic metastases, may be the first manifestation of an occult malignancy.

CT appearances. On CT, embolic metastases may produce thickening of the serosal surface of the bowel, which is often asymmetric and associated with bowel obstruction (Fig. 8a)^[42]. They may also appear as well-defined round masses within the peritoneal fat (Fig. 8b). Embolic metastases to

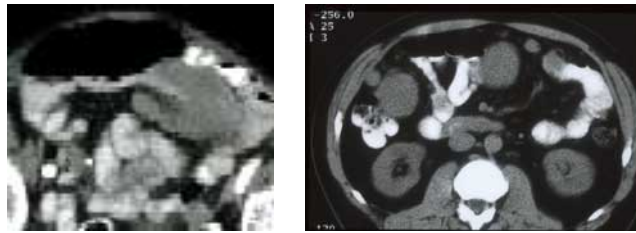


Figure 8 Embolic metastases. (a) Post contrast axial CT scan in a 60-year-old male with malignant melanoma showing a well defined embolic serosal deposits causing small bowel obstruction. (b) Axial CT scan in a 40-year-old male with leiomyosarcoma of the retroperitoneum showing multiple well defined soft tissue masses adjacent to the bowel in the mesenteric fat.

the stomach from breast cancer produces marked gastric wall thickening with almost complete obliteration of the lumen, an appearance that is indistinguishable from primary schirrous gastric carcinoma or lymphoma^[43].

CONCLUSION

Whilst most imaging appearances are non-specific and can also be mimicked by primary peritoneal malignancy and peritoneal inflammatory conditions, some peritoneal metastases have characteristic appearances. Understanding the complex peritoneal anatomy and the methods of spread may suggest the primary malignancy. The CT identification of peritoneal metastases has been correlated with second look laparotomy. The specificity of CT for the diagnosis of peritoneal metastases is high ranging from 85–87%, however its sensitivity is low, ranging from 42–47%^[45,46]. Laparoscopy has also demonstrated a significant incidence of peritoneal metastases in patients with a negative CT scan. Notably if ascites is present but no peritoneal deposits are seen on CT, laparoscopy demonstrated deposits in 75% of cases^[47]. At present CT remains the most useful imaging modality but recent MR technical developments allow similar accuracy in staging advanced disease.

REFERENCES

1. Oliphant M, Berne AS, Meyers MA. The subperitoneal space of the abdomen and pelvis: Planes of continuity. *AJR* 1996; 167: 1433–39.
2. Halvorsen RA, Panushka C, Oakley GJ *et al*. Intraperitoneal contrast material improves the CT detection of peritoneal metastases. *AJR* 1991; 157: 37–40.
3. Nelson RC, Chezmar JL, Hoel MJ, Buck DR, Sugarbaker PH. Peritoneal carcinomatosis: Preoperative CT with intraperitoneal contrast material. *Radiology* 1992; 182: 133–8.
4. Caseiro-Alves F, Goncalo M, Abraul E *et al*. Induced pneumoperitoneum in CT evaluation of peritoneal carcinomatosis. *Abdom Imaging* 1995; 20: 52–55.
5. Choi CK, Liu GC, Chen LT *et al*. MRI manifestations of peritoneal carcinomatosis. *Gastrointest Radiol* 1992; 17: 336–8.
6. Chou C-K, Liu G-C, Su J-H *et al*. MRI demonstration of peritoneal implants. *Abdominal Imaging* 1994; 19: 95.
7. Semelka RC, Lawrence PH, Shoenut JP, Heywood M, Kroeker MA, Lotocki R. Primary ovarian cancer: Prospective comparison of contrast enhanced CT and pre- and post-contrast, fat suppressed MR imaging, with histologic correlation. *J Mag Res Imaging* 1993; 3: 99–106.
8. Tempany CM, Zou KH, Silverman SG *et al*. Staging of advanced ovarian cancer: Comparison of imaging modalities — Report from the Radiology Diagnostic Oncology Group. *Radiology* 2000; 215: 761–7.
9. Derchi LE, Solbiati L, Rizziatto G *et al*. Normal anatomy and pathological changes of the small bowel mesentery: US appearance. *Radiology* 1987; 164: 649–52.
10. Goerg C, Schwerk W-B. Malignant ascites: Sonographic signs of peritoneal carcinomatosis. *Eur J Cancer* 1991; 27: 720–3.
11. Carrasquillo JA, Sugarbaker P, Colcher D *et al*. Peritoneal carcinomatosis: Imaging with intraperitoneal injection of I-131-labelled B72.3 monoclonal antibody. *Radiology* 1988; 167: 35–40.

12. Meyers MA, Oliphant M, Berne MS *et al.* The peritoneal ligaments and mesenteries: Pathways of intra-abdominal spread of disease. Annual oration. *Radiology* 1987; 163: 595–604.
13. Oliphant M, Berne A, Meyers MA. Subperitoneal spread of intra-abdominal disease. In *Computed tomography of the gastrointestinal tract including the peritoneal cavity and mesentery*. Edited by MA Myers. Springer Verlag, New York, 1986, pp. 95–137.
14. Balfe DM, Mauro MA, Koehler RE *et al.* Gastrohepatic ligament: Normal and pathologic CT anatomy. *Radiology* 1984; 150: 485–90.
15. Dehn CB, Reznick RH, Nockler B *et al.* The preoperative assessment of advanced gastric cancer by computed tomography. *Br J Surg* 1984; 71: 413–7.
16. Weinstein JB, Heiken JP, Lee JKT *et al.* High resolution CT of the porta hepatis and hepatoduodenal ligament. *Radiographics* 1986; 6(1): 55–73.
17. Baker ME, Silverman PM, Halvorsen RA *et al.* Computed tomography of masses in periportal/hepatoduodenal ligament. *J Comput Assist Tomogr* 1987; 11: 258–63.
18. Kim TK, Han JK, Chung JW, Choi BI, Park JH, Han MC. Intraperitoneal drop metastases from hepatocellular carcinoma: CT and angiographic findings. *J. Comput Assist Tomogr* 1996; 20(4): 638–42.
19. Ohtani T, Shirai Y, Tsukada K, Muto T, Hatakeyama K. Spread of gallbladder carcinoma: CT evaluation with pathologic correlation. *Abdom Imaging* 1996; 21(3): 195–201.
20. Diamond RT, Greenberg HM, Boulton IF. Direct metastatic spread of right colonic adenocarcinoma to duodenum: Barium and computed tomography findings. *Gastrointest Radiol* 1981; 6: 339–41.
21. McDaniel KP, Charnsangavej C, Du Brow *et al.* Pathways of nodal metastases in carcinomas of the cecum, ascending colon, and transverse colon. CT demonstration. *AJR* 1993; 160: 49–52.
22. Chun CH, Raff MF, Conteras L *et al.* Splenic abscess. *Medicine (Baltimore)* 1980; 59: 50–65.
23. Meyers MA. Distribution of intraabdominal malignant seeding: Dependency on dynamics of flow of ascitic fluid. *AJR* 1973; 119: 198–206.
24. Bergman F. Carcinoma of the ovary: A clinicopathological study of 86 autopsied cases with special reference to mode of spread. *Acta Obstet Gynaecol* 1966; 45: 211–31.
25. Dagnini G, Marin G, Caldironi MW *et al.* Laparoscopy in staging, follow-up, and re-staging ovarian carcinoma. *Gastrointest Endoscop* 1987; 33: 80–83.
26. Jeffrey RB Jr. CT demonstration of peritoneal implants. *AJR* 1980; 135: 323–6.
27. Buy J-N, Moss AA, Ghossain MA *et al.* Peritoneal implants from ovarian tumours: CT findings. *Radiology* 1988; 169: 691–4.
28. Megibow AJ, Bosniak MA, Ho AG *et al.* Accuracy CT in detection of persistent or recurrent ovarian carcinoma: Correlation with second look laparotomy. *Radiology* 1988; 166: 341–54.
29. Triller J, Goldnirsch A, Reinhard J-P. Subscapular liver metastases in ovarian cancer: Computer tomography and surgical staging. *Eur J Radiol* 1985; 5: 261–6.
30. Walkey MM, Friedman AC, Sohotra P *et al.* CT manifestations of peritoneal carcinomatosis. *AJR* 1988; 150: 1035–41.
31. Mitchell DG, Hill MC, Hill S *et al.* Serous carcinoma of the ovary: CT identification of metastatic calcified implants. *Radiology* 1986; 158: 649–52.
32. Matsuoka K, Okuhira M, Nonaka T *et al.* Calcification of peritoneal carcinomatosis from gastric carcinoma: a CT demonstration. *Eur J Radiol* 1991; 13: 207–8.
33. Woodard PK, Feldman JM, Paine SS, Baker ME. Midgut carcinoid tumours: CT findings and biochemical profiles. *J Comput Assist Tomogr* 1995; 19: 400–5.
34. Seshul MB, Coulam CM. Pseudomyxoma peritonei: Computed tomography and sonography. *AJR* 1981; 136: 803–6.
35. Whitley NO, Bohlman ME, Baker LP. CT patterns of mesenteric disease. *J Comput Assist Tomogr* 1982; 6: 490–6.
36. Cooper C, Jeffrey RB, Silverman PM *et al.* Computed tomography of omental pathology. *J Comput Assist Tomogr* 1986; 10: 62–6.
37. Pandolfo I, Blandino A, Gaeta M *et al.* Calcified peritoneal metastases from papillary cystadenocarcinoma of the ovary: CT features. *J Comput Assist Tomogr* 1986; 10: 545–6.
38. Tartar VM, Heiken JP, McClellan BL. Renal cell carcinoma presenting with diffuse peritoneal metastases: CT findings. *J Comput Assist Tomogr* 1991; 15(3): 450–3.
39. Cho KC, Gold BM. Computed Tomography of Krukenberg tumours. *AJR* 1985; 145: 285–86.
40. Goffinet DR, Castellino RA, Kim H *et al.* Staging laparotomies in unselected patients with non-Hodgkin's lymphoma. *Cancer* 1973; 32: 672–81.
41. Mueller PR, Ferrucci JT Jr, Harbin WP *et al.* Appearance of lymphomatous involvement of the mesentery by ultrasonography and body computer tomography: the 'sandwich sign'. *Radiology* 1980; 134: 467–73.

42. Kawashima A, Fishman EK, Kuhlman JE *et al.* CT of malignant melanoma: Patterns of small bowel and mesenteric involvement. *J Comput Assist Tomogr* 1991; 15(4): 570–4.
43. Caskey CI, Scatarige JC, Fishman EK. Distribution of metastases in breast carcinoma. CT evaluation of the abdomen. *Clin Imaging* 1991; 15: 166–71.
44. Oddson TA, Rice RRP, Seiler HF *et al.* The spectrum of small bowel melanoma. *Gastrointest Radiol* 1978; 3: 419–23.
45. Pectasides D, Kayianni H, Facou A *et al.* Correlation of abdominal computed tomography scanning and second look operation findings in ovarian cancer patients. *Am J Clin Oncol* 1991; 14: 457–62.
46. De-Rosa V, Mangoni-di-Stefano ML, Brunetti A *et al.* Computed tomography and second-look surgery in ovarian cancer patients. Correlation, actual role and limitations of CT scan. *Eur J Gynaecol Oncol* 1995; 16: 123–9.
47. Brady PG, Peebles M, Goldschmid S. Role of laparoscopy in the evaluation of patients with suspected hepatic or peritoneal malignancy. *Gastrointest Endosc* 1991; 37: 27–30.